The 2010 IEEE/RSJ International Conference on
Intelligent Robots and Systems
October 18-22, 2010, Taipei, Taiwan

Position Control Methods of Spherical Ultrasonic Motor

Naoyuki Takesue, Tomohiro Ohara, Ryota Ishibashi, Shigeki Toyama, Masahiko Hoshina, Yoshiyuki Hirai, Naoki Fukaya, Jumpei Arata, and Hideo Fujimoto

Abstract— **In this paper, we investigate the position control of spherical ultrasonic motor (SUSM). The generated torque of SUSM is influenced by the phase difference and the driving frequency of applied AC voltages. Therefore, the control strategy is classified into three types: (a) variable phase and fixed frequency, (b) fixed phase and variable frequency, and (c) variable phase and frequency. We formulate the position control rules for SUSM based on the above three types of control variables, and investigate the performances experimentally.**

I. INTRODUCTION

Spherical motor is one of the multi-DOF actuators, and the promising applications are robot manipulator[1], actuator for a camera on robot[2], [3], mobile robot[4], [5], haptic device[6] and so on.

An ultrasonic motor[7] has several advantages such as a high output torque at low speed without a reduction gear, holding torque for braking, and high responsiveness. Also, it has a capability to construct the multi-DOF actuator with a compact and simple structure, as in [8], [9], [10].

A spherical ultrasonic motor (SUSM), which has the above advantages, has been developed and studied[8], [11], [12]. In order to control the position of SUSMs, several position control methods have been studied[2], [8], [11]. For example, Ref.[2] has proposed the hybrid control using the phase difference and frequency of input voltages. Ref.[8] has conducted the trajectory control. Ref.[11] has mentioned that the phase difference is changed for the position control. However, they have not formulated the control rules enough and clarified the differences of those control performances. In order to realize the better performance, the investigation of the position control methods of SUSM is required.

The generated torque of SUSM is influenced by the phase difference and the driving frequency. Therefore, the torque control strategy is classified into three types: (a) variable phase and fixed frequency, (b) fixed phase and variable frequency, and (c) variable phase and frequency.

The purpose of this study is to formulate the position control strategy for SUSM based on the above three types of control variables, and to investigate the performances. The rest of this paper is organized as follows. Section II depicts the principle of SUSM and the classification of the torque control strategy of SUSM. Section III describes three kinds of position control methods based on the torque control strategy. Section IV demonstrates the experimental system and the experimental results. Finally, Section V provides the conclusions and future works.

N. Takesue and T. Ohara are with Graduate School of System Design, Tokyo Metropolitan University, Tokyo, Japan.
ntakesue@sd.tmu.ac.jp
R. Ishibashi, J. Arata and H. Fujimoto are with Nagoya Institute of Technology, Nagoya, Aichi, Japan
S. Toyama, M. Hoshina and Y. Hirai are with Department of Mechanical Systems Engineering Department, Tokyo University of Agriculture and Technology, Tokyo, Japan.
N. Fukaya is with Tokyo Metropolitan College of Industrial Technology, Tokyo, Japan.

II. SPHERICAL ULTRASONIC MOTOR

A. Principle of Spherical Ultrasonic Motor

The SUSM used in this study consists of one spherical rotor and three ring-shaped stators. Figure 1 shows an overview of the SUSM. The geometric schemes are illustrated in Fig. 2.

The stator includes a metallic elastic body and piezoelectric elements. When an AC voltage is applied to the piezoelectric vibrator, a standing wave is generated on the elastic body. By applying two AC voltages with a phase difference to the positive and negative sections of the piezoelectric elements, a traveling wave is generated due to combination

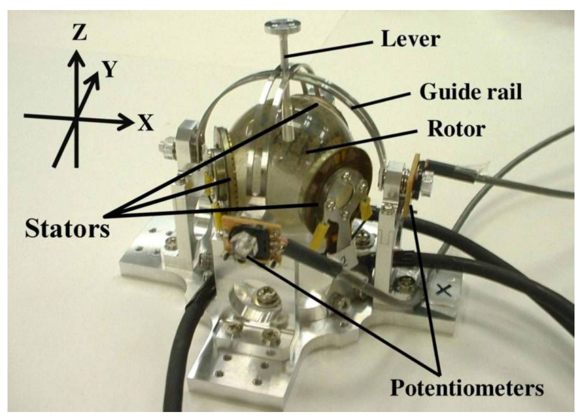

Fig. 1. Spherical ultrasonic motor used in this study

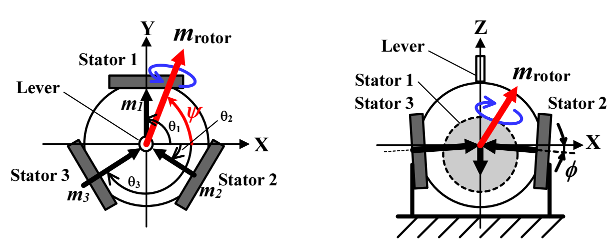

(a) Geometry from top view (b) Geometry from top view

Fig. 2. Geometric scheme of SUSM

978-1-4244-6676-4/10/$25.00 ©2010 IEEE

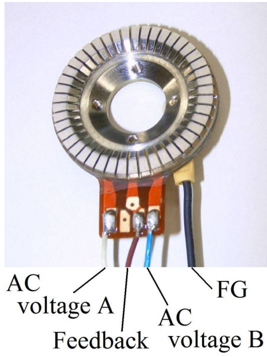

Fig. 3. Single stator

of the two standing waves[7]. The stators and the rotor are in pressure contact with each other, and the rotor is driven by the tangential force of the elliptical motion of the traveling wave. A single stator is shown in Fig. 3. Another piezoelectric element on the stator is used as a sensor detecting the resonance, and the signal is called the feedback signal. There are two inputs (AC voltage A and B), one output (Feedback) and FG (Frame Ground) terminals.

The stators, namely vibrators, are located as shown in Fig. 2. Geometric parameters (stators' alignment) are θ_1, θ_2, θ_3 and ϕ. Using the parameters, the moment vector of each stator, $\boldsymbol{m}_i$, can be expressed as follows:

$$\boldsymbol{m}_i = \begin{bmatrix} -\cos\theta_i \cos\phi \\ -\sin\theta_i \cos\phi \\ \sin\phi \end{bmatrix} \tau_i, \quad (i = 1,\, 2,\, 3) \tag{1}$$

Here, τ_i is the generated torque of each stator.

As a result, the output moment vector of the rotor, $\boldsymbol{m}_{\text{rotor}}$, can be described as the summation of the vectors $\boldsymbol{m}_i$ in Eq. (1).

$$\begin{aligned} \boldsymbol{m}_{\text{rotor}} &= \begin{bmatrix} m_x \\ m_y \\ m_z \end{bmatrix} = \boldsymbol{m}_1 + \boldsymbol{m}_2 + \boldsymbol{m}_3 \\ &= \begin{bmatrix} -\mathrm{c}\theta_1\mathrm{c}\phi & -\mathrm{c}\theta_2\mathrm{c}\phi & -\mathrm{c}\theta_3\mathrm{c}\phi \\ -\mathrm{s}\theta_1\mathrm{c}\phi & -\mathrm{s}\theta_2\mathrm{c}\phi & -\mathrm{s}\theta_3\mathrm{c}\phi \\ \mathrm{s}\phi & \mathrm{s}\phi & \mathrm{s}\phi \end{bmatrix} \begin{bmatrix} \tau_1 \\ \tau_2 \\ \tau_3 \end{bmatrix} \\ &= D\boldsymbol{\tau} \quad . \end{aligned} \tag{2}$$

Here, $\mathrm{s}\theta_i = \sin\theta_i$, $\mathrm{c}\theta_i = \cos\theta_i$, $\mathrm{s}\phi = \sin\phi$, $\mathrm{c}\phi = \cos\phi$, and D is a constant matrix. From the Eq. (2), we can control the moment of rotor, $\boldsymbol{m}_{\text{rotor}}$, with the torque of stators, $\boldsymbol{\tau}$.

B. Stator Torques Required for Rotor Moment

In this subsection, we derive the stator torques that require to realize the desired moment $\boldsymbol{m}_d$. In the posture control strategy, we rotate the SUSM to the target position along the moment $\boldsymbol{m}_d$. From the Eq. (2), the required stator torque $\boldsymbol{\tau}$ can be obtained as follows:

$$\boldsymbol{\tau} = D^{-1}\boldsymbol{m}_d \quad . \tag{3}$$

Since the geometric parameter ϕ is nearly zero in the used SUSM, we premeditate such the 2DOF motion so that m_z can be neglected, and we obtain the following relationship.

$$\boldsymbol{\tau} = \frac{1}{d\,\mathrm{c}\phi} \begin{bmatrix} \mathrm{s}\theta_2 - \mathrm{s}\theta_3 & -\mathrm{c}\theta_2 + \mathrm{c}\theta_3 \\ \mathrm{s}\theta_3 - \mathrm{s}\theta_1 & -\mathrm{c}\theta_3 + \mathrm{c}\theta_1 \\ \mathrm{s}\theta_1 - \mathrm{s}\theta_2 & -\mathrm{c}\theta_1 + \mathrm{c}\theta_2 \end{bmatrix} \begin{bmatrix} m_x \\ m_y \end{bmatrix} \tag{4}$$

where, $d = \sin(\theta_1 - \theta_2) + \sin(\theta_2 - \theta_3) + \sin(\theta_3 - \theta_1)$.

As shown in Fig. 2(a), geometry of the each stator becomes $\theta_1 = \pi/2$, $\theta_2 = -\pi/6$ and $\theta_3 = -5\pi/6$, and the Eq. (4) can be expressed as follows:

$$\begin{aligned} \boldsymbol{\tau} &= \frac{2}{3\sqrt{3}\,\mathrm{c}\phi} \begin{bmatrix} 0 & -\sqrt{3} \\ -3/2 & \sqrt{3}/2 \\ 3/2 & \sqrt{3}/2 \end{bmatrix} \begin{bmatrix} m_x \\ m_y \end{bmatrix} && (5) \\ &= -\frac{2}{3\,\mathrm{c}\phi} \begin{bmatrix} \cos\left(\frac{\pi}{2}\right) & \sin\left(\frac{\pi}{2}\right) \\ \cos\left(-\frac{\pi}{6}\right) & \sin\left(-\frac{\pi}{6}\right) \\ \cos\left(-\frac{5\pi}{6}\right) & \sin\left(-\frac{5\pi}{6}\right) \end{bmatrix} \begin{bmatrix} m_x \\ m_y \end{bmatrix} && (6) \\ &= \frac{2\,\|\boldsymbol{m}_d\|}{3\,\mathrm{c}\phi} \begin{bmatrix} \sin(\psi' - \theta_1) \\ \sin(\psi' - \theta_2) \\ \sin(\psi' - \theta_3) \end{bmatrix} \quad , && (7) \end{aligned}$$

where, $\psi = \mathrm{atan2}(m_y,\, m_x)$ is the direction of the target moment $\boldsymbol{m}_d$ on the X-Y plane, and $\psi' = \psi - \pi/2$ is the direction of the motion of lever as shown in Fig. 4(a). $\|\boldsymbol{m}_d\| = \sqrt{m_x^2 + m_y^2}$ is a norm of the moment.

C. Torque Control Strategy of Stator

Generally, the single stator torque can be expressed as

$$\tau_i = c_i(f_i) \sin\rho_i, \tag{8}$$

where, f_i is the frequency and ρ_i is the phase difference of two AC voltages (A and B). Here, $c_i(f_i)$ is a magnitude of torque, a function of the f_i. When f_i to be tuned to resonant frequency $f_{\text{res},i}$, $c_i(f_i)$ becomes maximum value, $c_{\max,i}$. Thus, we can obtain maximum value of the stator torque when the system satisfies the following condition.

$$f_i = f_{\text{res},i}, \text{ and } \rho_i = \pm\pi/2. \tag{9}$$

Eq. (7) expresses the relationship between desired moment and stator torque. On the other hand, Eq. (8) means that there are two ways to control the stator torque: the frequency and the phase difference. Thus, it is possible to classify the torque control strategy into three kinds of methods as follows.

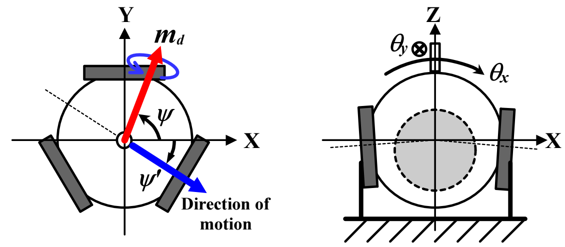

(a) Top view (b) Side view

Fig. 4. Relationship of moment and direction of motion

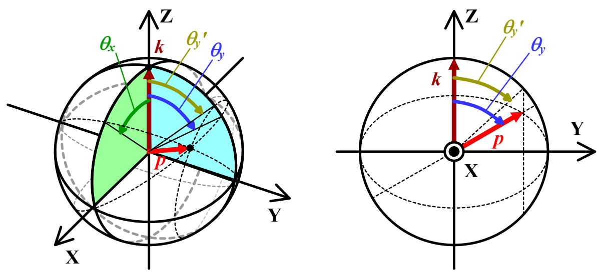

Fig. 5. Angles and Position of lever

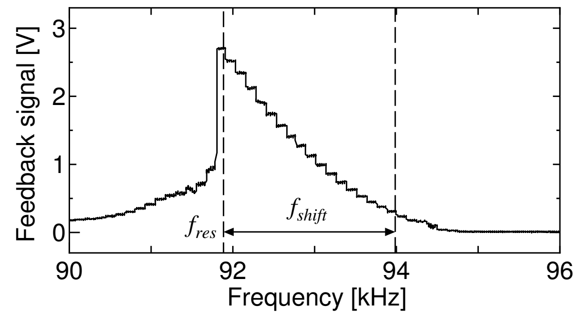

Fig. 6. Feedback signal vs. Frequency

1) Torque Control Based on Phase Difference (PH): Let the frequency f_i be the resonant frequency $f_{\text{res},i}$, and $c_{\max,i} = \frac{2\,m_{\max}}{3\,c\phi}$. Here, $m_{\max}$ is the maximum absolute value of the moment of rotor. Then, we can generate the target torque when the phase difference ρ_i satisfies a following condition.

$$\begin{cases} c_i(f_i) = c_{\max,i} = \dfrac{2\,m_{\max}}{3\,c\phi} \\ \sin\rho_i = \dfrac{\|\boldsymbol{m}_d\|}{m_{\max}} \sin(\psi' - \theta_i) \end{cases} \tag{10}$$

We refer this type of torque control *PH method* in this paper.

If Eq. (10) is substituted into Eq. (8), Eq. (7) can be obtained.

2) Torque Control Based on Frequency (FR): When we settle the phase difference ρ_i as $\rho_i = \pi/2$ or $\rho_i = -\pi/2$, —switches according to the direction of required torque—, we can generate the target torque with the frequency f_i.

$$\begin{cases} c_i(f_i) = \dfrac{2\,\|\boldsymbol{m}_d\|}{3\,c\phi} |\sin(\psi' - \theta_i)| \\ \sin\rho_i = \text{sgn}\{\sin(\psi' - \theta_i)\} \end{cases} \tag{11}$$

This type of torque control is referred as *FR method*.

3) Torque Control Based on Phase Difference and Frequency (HB): We control both the phase difference and the frequency with Eq. (8). That is, we control f_i and ρ_i using a following condition.

$$\begin{cases} c_i(f_i) = \dfrac{2\,\|\boldsymbol{m}_d\|}{3\,c\phi} \\ \sin\rho_i = \sin(\psi' - \theta_i) \end{cases} \tag{12}$$

This may be called a hybrid control[2] (in this paper, refer to *HB method*).

III. Position Control of SUSM

A. Kinematics between Sensor Angle and Rotor Position

A picture of the SUSM used in this study was shown in Fig. 1. Potentiometers shown in the figure measure the angle of the lever (θ_x, θ_y) via guide rails (see Fig. 4(b) and Fig. 5). θ_x and θ_y are the angles between the axis Z and the lever projected on the X-Z plane and the Y-Z plane, respectively.

On the other hand, we express the position of lever as the posture of vector. The original position vector of the lever is set to $\boldsymbol{k} = [0,\,0,\,1]^T$ when it corresponds to Z-axis. The position vector of the lever $\boldsymbol{p}$ is expressed as follows:

$$\boldsymbol{p} \;=\; R_y(\theta_x) R_x(\theta_y') \boldsymbol{k} \quad , \tag{13}$$

where, $R_x(\theta)$ means the rotation matrix around the axix x through an angle of θ. By solving the above equations, when the angles θ_x and θ_y are obtained from the potentiometers, the position vector of the lever, $\boldsymbol{p}$, is expressed as follows:

$$\boldsymbol{p} \;=\; \begin{bmatrix} \sin\theta_x\,\cos\theta_y' \\ \sin\theta_y' \\ \cos\theta_x\,\cos\theta_y' \end{bmatrix} \quad , \tag{14}$$

where $\theta_y' = \tan^{-1}\{\cos\theta_x\,\tan\theta_y\}$.

B. Driving Frequency and Feedback Signal

Figure 6 shows an example of feedback signal obtained from a single stator while changing the driving frequency. As seen from this figure, the resonant frequency of the stator (vibrator) $f_{\text{res},i}$ is about 92 [kHz].

The sudden change is observed at the lower frequencies than the resonant frequency. On the other hand, at the higher frequency, the feedback signal changes gently[8]. Therefore, it can be thought that the generated torque of the stator is changed smoothly along with shifting the driving frequency to the higher frequency. In the figure, the frequency should be changed between 92 and 94 [kHz].

C. Position Control Methods

1) Desired Moment Vector: The desired moment vector $\boldsymbol{m}_d$ that approaches the position vector of the lever $\boldsymbol{p}$ to the target position vector $\boldsymbol{p}_d$ can be written as the following equation:

$$\boldsymbol{m}_d = \begin{cases} \boldsymbol{0} & \text{if } \|\boldsymbol{p} \times \boldsymbol{p}_d\| = 0 \\ k(\alpha)\,\dfrac{\boldsymbol{p} \times \boldsymbol{p}_d}{\|\boldsymbol{p} \times \boldsymbol{p}_d\|} & \text{otherwise} \end{cases} \quad , \tag{15}$$

where $\alpha \geq 0$ is the angle between $\boldsymbol{p}$ and $\boldsymbol{p}_d$. $k(\alpha)$ is the absolute value of the moment vector (torque) expressing as a function of the angle α. The absolute value of $\boldsymbol{m}_d$ is $\|\boldsymbol{m}_d\| = k(\alpha)$. Because the actual torque has an upper limitation, the maximum value becomes $\max\{k(\alpha)\} = m_{\max}$.

For example, in the case where the torque is proportional to the angle α, the value is simply expressed as below:

$$k(\alpha) = K_P\,\alpha \quad , \tag{16}$$

where K_P is the proportional gain.

On the other hand, when the upper limitation (saturation) is considered, the value is expressed as follows:

$$k(\alpha) \;=\; \begin{cases} K_P\,\alpha & \text{if } \alpha < \alpha_{\text{th}} \\ m_{\max} & \text{otherwise} \end{cases} \quad . \tag{17}$$

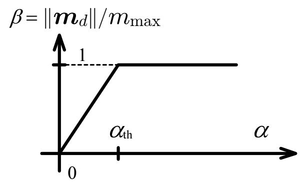

Fig. 7. Gain β vs. Angular Error α

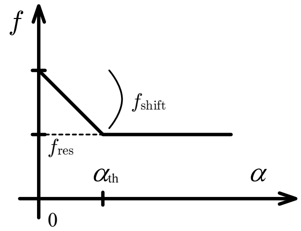

Fig. 8. Frequency f vs. Angular Error α

Here, $\alpha_{\text{th}} = m_{\max}/K_P$ is a threshold angle of the torque saturation.

Furthermore, β is defined to normalize with $m_{\max}$.

$$k(\alpha) = \beta\, m_{\max} \tag{18}$$

$$\beta = \begin{cases} \alpha/\alpha_{\text{th}} & \text{if } \alpha < \alpha_{\text{th}} \\ 1 & \text{otherwise} \end{cases} \tag{19}$$

This condition can be illustrated as Fig. 7. The slope $1/\alpha_{\text{th}}$ is relative to the proportional gain K_P.

In the above, only the proportional (P) control is considered for simplicity. It can, of course, include the integral (I) control and/or the derivative (D) control as well.

2) PH Method: According to II-C.1, the driving frequency f_i is set to the predetermined resonant frequency $f_{\text{res},i}$, and the phase difference ρ_i is varied in order to control the rotor position. The second equation of Eq. (10), which is about the phase, can be rewritten as below based on Eq. (19).

$$\sin\rho_i = \beta \sin(\psi' - \theta_i) \tag{20}$$

3) FR Method: Based on II-C.2, the phase difference is fixed as $\rho = \pm\pi/2$, the driving frequency f_i is varied. Although it is not easy to obtain the relation of $c_i(f_i)$ practically, it is assumed that the torque is proportional to the frequency[8]. Then, the control rule can be described as:

$$f_i = f_{\text{res},i} + f_{\text{shift},i}(1 - \beta\,|\sin(\psi' - \theta_i)|) \tag{21}$$

$$\sin\rho_i = \text{sgn}\{\sin(\psi' - \theta_i)\} \tag{22}$$

4) HB Method: According to II-C.3, both phase and frequency are changed. The phase can be obtained from the second equation of Eq. (12). On the other hand, the driving frequency is expressed similarly to the FR method.

$$f_i = f_{\text{res},i} + f_{\text{shift},i}(1 - \beta) \tag{23}$$

$$\sin\rho_i = \sin(\psi' - \theta_i) \tag{24}$$

For example, in case of Fig. 6, $f_{\text{res},i} \simeq 92$ [kHz] and $f_{\text{shift},i} \simeq 2$ [kHz]. The above equation is illustrated as Fig. 8.

IV. EXPERIMENTS

A. Experimental System

The system configuration in this study is shown in Fig. 9. The feedback signals of stators and the potentiometer voltages are measured with A/D converter. The position of lever on the rotor is calculated from the potentiometer voltages. From the difference between present and target positions, the desired moment is obtained. Finally, in order to realize the torque, the driving frequencies and phase differences of stators are determined by PH, FR or HB method, and they are set to the driver of SUSM.

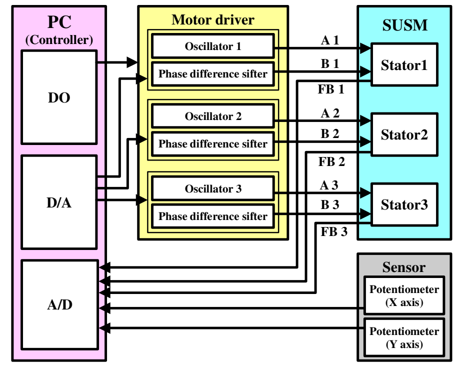

Fig. 9. System configuration

An example of the control procedure based on PH method is presented as follows:

1) The control gain $K_P = 1/\alpha_{\text{th}}$ is predetermined.
2) The target position $\boldsymbol{p}_d$ is set to a certain position.
3) The current position $\boldsymbol{p}$ is calculated from Eq. (14) with the angles θ_x and θ_y measured by the potentiometers.
4) The angle α is obtained from $\boldsymbol{p}_d$ and $\boldsymbol{p}$. Namely, β is calculated from Eq. (19).
5) The driving frequency, f_i, is fixed to $f_{\text{res},i}$, and the phase difference ρ_i is calculated from Eq. (20).
6) Two AC voltages with the frequency f_i and the phase difference ρ_i are input to each stator.
7) Continue (back to 3) procedure).

These procedure is conducted at a sampling time of 1 [ms] by PC with ART-Linux[13].

B. Step Responses

The step response experiments are examined using the control methods mentioned in the previous section. The desired angle of Y-axis is zero, and the desired angle of X-axis θ_{xd} is selected as ± 1, 3, 5 [deg] since larger θ_{xd} tends to occur the saturation. The threshold α_{th} was changed to 1, 3 and 10 [deg], which is determined on trial-and-error. As a result, $\alpha_{\text{th}} = 3$ [deg] exhibits the best responses. Therefore, the results shown below are the ones in case of $\alpha_{\text{th}} = 3$ [deg]. The step responses with PH, FR and HB methods are shown in Figs. 10 to 12, respectively.

In the PH method (Fig. 10), at the steady state, the fluctuations and error are observed. In the FR method (Fig. 11), the fast responsiveness and a small error are demonstrated at the steady state. On the other hand, noisy response is also observed. In the HB method (Fig. 12), a good stability and small error are shown.

C. Circular Trajectory

By using the three methods, we make the SUSM trace a circular trajectory of radius of 3 [deg]. The periodic time is 4 [s]. The experimental results are shown in Figs. 13 to 15, respectively.

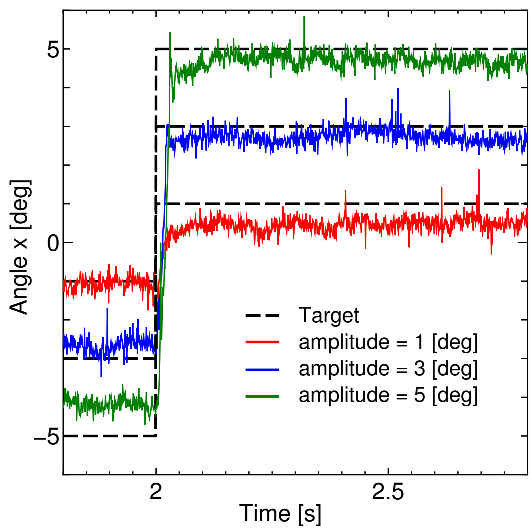

Fig. 10. Step responses (PH)

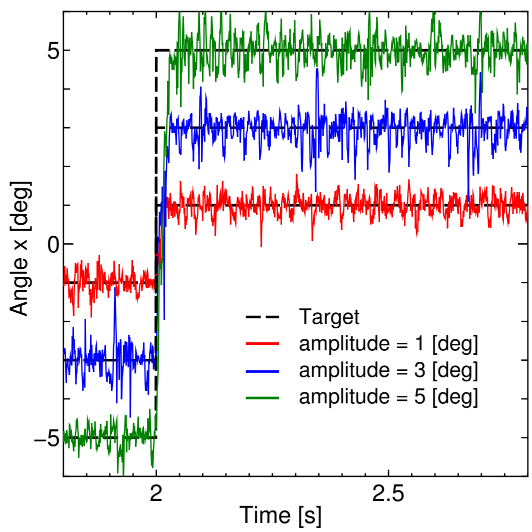

Fig. 11. Step responses (FR)

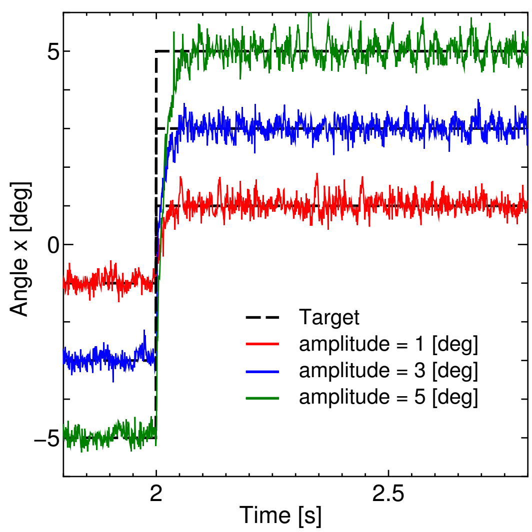

Fig. 12. Step responses (HB)

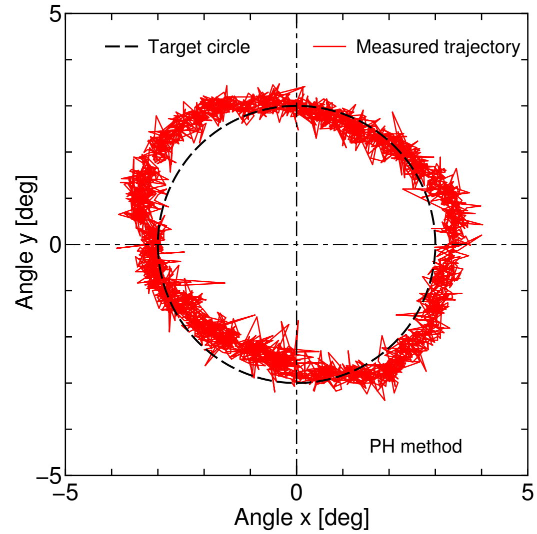

Fig. 13. Circular Trajectory (PH) of Radius 3 [deg]

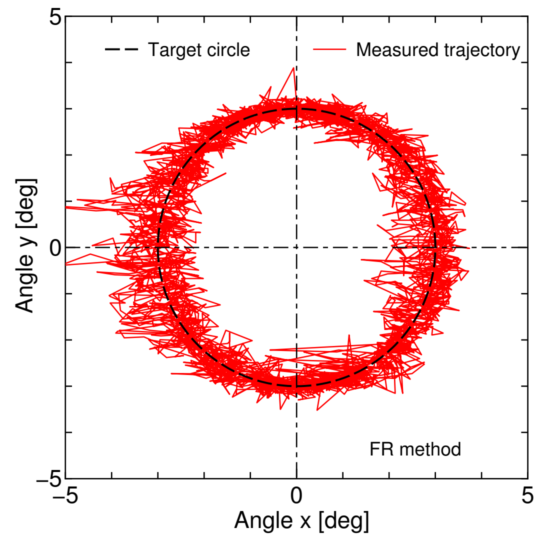

Fig. 14. Circular Trajectory (FR) of Radius 3 [deg]

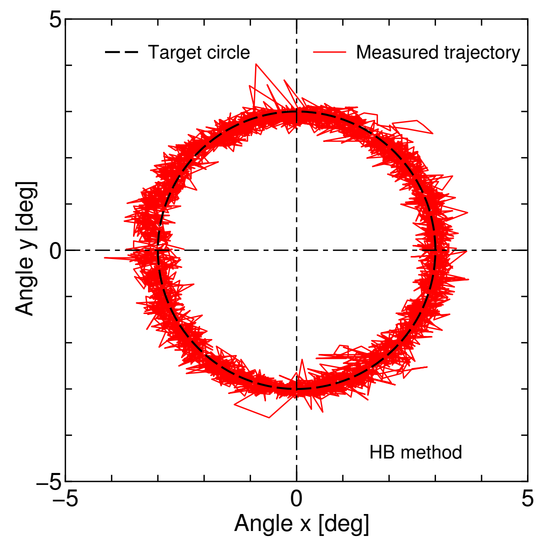

Fig. 15. Circular Trajectory (HB) of Radius 3 [deg]

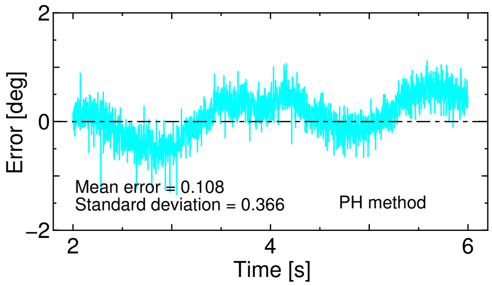

Fig. 16. Error of Circular Trajectory (PH)

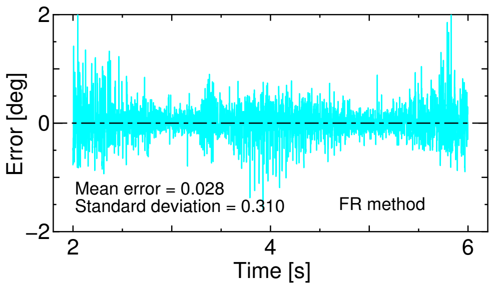

Fig. 17. Error of Circular Trajectory (FR)

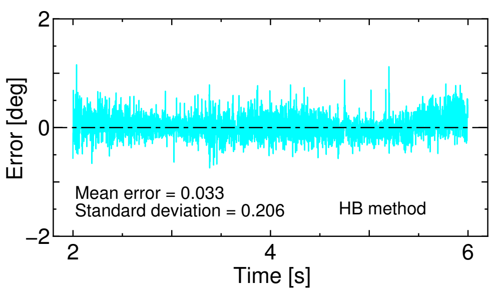

Fig. 18. Error of Circular Trajectory (HB)

TABLE I
MEAN ERROR AND STANDARD DEVIATION

Method	Mean Error [deg]	Standard Deviation [deg]
PH	0.108	0.366
FR	0.028	0.310
HB	0.033	0.206

The result of PH method shows large error as seen from the step response. On the other hand, FR and HB methods trace the target circle with small error. Figs. 16 to 18 show the error from the target circle. And the mean error and the standard deviation of each methods are shown in Table I. As seen from the figures and table, HB method, in this experiment, has shown the lowest error and deviation.

D. Discussion

The PH method is influenced by the characteristics of the phase difference. As seen from the characteristics of rotational speed and phase in [2], it exhibits nearly sinusoidal relationship. However, it may have lost motion and asymmetric diversity. The steady state error may be caused by the characteristics. Since the error can be reduced by adding the integral control, it is not a large problem.

The FR and HB methods have not only $\alpha_{\rm th}$, but also $f_{{\rm shift},i}$ as the control parameters. In the above experiments, the same $\alpha_{\rm th}$ and $f_{{\rm shift},i}$ are applied. However, they can be tuned for better responses.

V. CONCLUSIONS AND FUTURE WORKS

A. Conclusions

In this paper, the classification and formulation of the position control strategy of SUSM are shown. The three methods, namely PH, FR and HB methods, are implemented. The position control experiments are conducted and the control performances are investigated.

PH method exhibits the steady state error and fluctuation. FR and HB methods show the faster response and lower error than PH method does although they include noisy response.

B. Future Works

This paper treats only the proportional control with constant parameters. The investigation of PID control performance and their parameters (gains, $\alpha_{\rm th}$ and $f_{{\rm shift},i}$) tuning in detail must be a future work.

VI. ACKNOWLEDGMENTS

Part of this study was funded by NEDO P10003 "Intelligent Surgical Instruments Project", Japan.

REFERENCES

[1] N. Fukaya, S. Toyama, T. Asfour and R. Dillmann: "Design of the TUAT/Karlsruhe Humanoid Hand," Proc. 2000 IEEE/RSJ International Conference on Intelligent Robots and Systems (IROS 2000), pp.1754-1759, 2000.

[2] M. Hoshina, T. Mashimo, and S. Toyama: "Development of Spherical Ultrasonic Motor as a Camera Actuator for Pipe Inspection Robot," Proc. of 2009 IEEE/RSJ International Conference on Intelligent Robots and Systems (IROS 2009), pp.2379-2384, 2009.

[3] M. Hoshina, T. Mashimo, S. Toyama: "Development of Pipe Inspection Robot; Driving System and Control of Outer-rotor-typed Spherical Ultrasonic Motor," Proc. International Conference on Advanced Robotics (ICAR 2009), pp.97-102, 2009.

[4] T. B. Lauwers, G. A. Kantor, and R. L. Hollis: "A Dynamically Stable Single-Wheeled Mobile Robot with Inverse Mouse-Ball Drive," Proc. IEEE Int. Conf. on Robotics and Automation (ICRA 2006), pp.2884-2889, 2006.

[5] M. Kumagai, T. Ochiai: "Development of a robot balanced on a ball: application of passive motion to transport," Proc. IEEE Int. Conf. on Robotics and Automation (ICRA 2009), pp.916-921, 2009.

[6] L. Birglen, C. Gosselin, N. Pouliot, B. Monsarrat, and T. Laliberté: "SHaDe, A New 3-DOF Haptic Device," IEEE Trans. on Robotics and Automation, vol.18, no.2, pp.166-175, 2002.

[7] T. Sashida and T. Kenjo: "An introduction to ultrasonic motors," Oxford Press, 1993.

[8] S. Toyama, S. Sugitani, G. Zhang, Y. Miyatani, and K. Nakamura: "Multi degree of freedom Spherical Ultrasonic Motor," Proc. of 1995 IEEE International Conference on Robotics and Automation (ICRA 1995), pp.2935-2940, 1995.

[9] T. Amano, T. Ishii, K. Nakamura and S. Ueda: "An Ultrasonic Actuator with Multi-Degree of Freedom using Bending and Longitudinal Vibrations of a Single Stator," Proc. IEEE Int. Ultrasonics Symp., pp.667-670, 1998.

[10] K. Takemura and T. Maeno: "Design and Control of an Ultrasonic Motor Capable of Generating Multi-DOF Motion," IEEE/ASME Trans. on Mechatronics, Vol.6, no.4, pp.499-506, 2001.

[11] E. Purwanto and S. Toyama: "Control Method of a Spherical Ultrasonic Motor," Proc. of 2003 IEEE/ASME International Conference on Advanced Intelligent Mechatronics (AIM 2003), pp.1321-1326, 2003.

[12] X. Hu, J. Guo, R. Shen: "Modeling and Performance Evaluation of 2DOF Spherical Traveling-wave Type Ultrasonic Motor," Proc. of International Conference on Electrical Machines and Systems (ICEMS 2008), pp.3831-3834, 2008.

[13] http://www.dh.aist.go.jp/en/research/humanoid/ART-Linux/